

Contents lists available at ScienceDirect

Heliyon

journal homepage: www.cell.com/heliyon



Research article



Variation the in relationship between urban tree canopy and air temperature reduction under a range of daily weather conditions

Dexter Henry Locke ^{a,*}, Matthew Baker ^b, Michael Alonzo ^c, Yichen Yang ^d, Carly D. Ziter ^e, Colleen Murphy-Dunning ^f, Jarlath P.M. O'Neil-Dunne ^g

- a USDA Forest Service, Northern Research Station, Baltimore Field Station, Suite 350, 5523 Research Park Drive, Baltimore, MD, 21228, USA
- b Department of Geography & Environmental Systems, University of Maryland Baltimore County, 1000 Hilltop Circle, Baltimore, MD, 21250, USA
- ^c Department of Environmental Science, American University, Hall of Science 328 4400 Massachusetts Ave, NW Washington, DC, 20016-8014, USA
- ^d Yale School of the Environment, Environmental Science Center, Room 300, 21 Sachem Street, New Haven, CT, 06511, USA
- e Department of Biology, Concordia University, 7141 Sherbrooke West, Montreal, Quebec, H4B 1R6, Canada
- f Hixon Center Urban Sustainabilitiy, Urban Resources Initiative, Yale School of the Environment, 301 Prospect St #1, New Haven, CT, 06511, USA
- g Spatial Analysis Lab, Rubenstein School of Environment and Natural Resources, University of Vermont, 81 Carrigan Drive, Burlington, VT, 05405, USA

ARTICLE INFO

Keywords: Urban heat island Mobile sampling Distributed network Air temperature Bicycles Tree canopy

ABSTRACT

Mitigating heat is a vital ecosystem service of trees, particularly with climate change. Land surface temperature measures captured at a single time of day (in the morning) dominate the urban heat island literature. Less is known about how local tree canopy and impervious surface regulate air temperature throughout the day, and/or across many days with varied weather conditions, including cloud cover. We use bike-mounted air temperature sensors throughout the day in New Haven, Connecticut, USA, from 2019 to 2021 and generalized additive mixed models across 156 rides to estimate the daily variation in cooling benefits associated with tree canopy cover, and warming from impervious surface cover in 90 m buffers surrounding bike observations. Cooling is inferred by subtracting the bicycle-observed temperature from a reference station. The cooling benefits from tree canopy cover were strongest in the midday (11:00–14:00, -1.62 °C), afternoon (14:00–17:00, -1.19 °C), and morning (8:00–11:00, -1.15 °C) on clear days. The cooling effect was comparatively smaller on cloudy mornings -0.92 °C and afternoons -0.51 °C. Warming from impervious surfaces was most pronounced in the evening (17:00-20:00, 1.11 °C) irrespective of clouds, and during cloudy nights (20:00-23:00) and cloudy mornings 1.03 °C 95 % CI [1.03, 1.04]. Among the hottest observed days (top 25th percentile of reference station daily maxima), tree canopy was associated with lower temperatures on clear afternoons -1.78 °C [-1.78, -1.78], cloudy midday $-1.17 \,^{\circ}$ C [-1.19, -1.15], clear midday $-1.12 \,^{\circ}$ C [-1.12, -1.11]. We add a broader spectrum of weather conditions by explicitly including clouds, and greater temporal resolution by measuring throughout the day to bike-based urban heat research. Future mobile sampling campaigns may broaden the spatial extent with more environmental variation, representing an opportunity for public science and engagement.

E-mail addresses: dexter.locke@gmail.com, dexter.locke@usda.gov (D.H. Locke), mbaker@umbc.edu (M. Baker), alonzo@american.edu (M. Alonzo), yichen.yang@yale.edu (Y. Yang), carly.ziter@concordia.ca (C.D. Ziter), colleen.murphy-dunning@yale.edu (C. Murphy-Dunning), jarlath.ONeil-Dunne@uvm.edu (J.P.M. O'Neil-Dunne).

https://doi.org/10.1016/j.heliyon.2024.e25041

^{*} Corresponding author.

1. Introduction

Trees are an important part of urban ecosystems in temperate, forested regions due to their capacity for providing ecosystem services [1,2]. Trees help mitigate the lethality [3,4] of the worsening urban heat island effect from climate change [5] through shading [6–8] and evapotranspiration [7,9]. The effects of these different cooling mechanisms vary across space and over time [10,11], and interact with other aspects of the built environment [8,12–15] and regional meteorology [16].

The well-described urban heat island (UHI) effect is the phenomenon where urbanized areas are hotter than their rural and suburban counterparts [17,18]. This effect is due to the prevalence of impervious, dense surfaces that absorb, store, and re-radiate heat, combined with the lack of vegetative cover that cools through transpiration, and shades surfaces to prevent them from getting hot in the first place [8,9,12]. Although spatial patterns of inter- and intra-urban surface temperature and inequity are well documented [19, 20], less is known about spatio-temporal variability in air temperatures as they relate to urban land cover. The variable effects of tree canopy and impervious surface on air temperature throughout any relatively warm day, or across many days with varied cloud cover remains poorly understood [21].

Research on urban vegetation and urban heat frequently focuses on land surface temperature representing a single time of day [19, 20,22–26]. Due to its orbit, Landsat-based work in the contiguous United States measures surface temperature between 10 and 11 a.m. in the morning, before temperatures reach their daily maximum. Remotely sensed estimates of surface temperature are further hindered by clouds. Cloudy images are usually removed from analyses, challenging the ability to measure land cover-temperature relationships under cloudy conditions. Extrapolating land surface temperature via statistical and/or physical models introduces substantial uncertainty [27,28].

Land surface temperatures did not correspond well to air temperatures recorded from fixed-location sensors in either Vancouver, Canada [13] or Rotterdam, The Netherlands [29]. Air temperature is a more salient measure for human health than surface temperature [30], even though it is more challenging to obtain. Yet spatially extensive, ground-level air temperature monitoring remains rare in urban areas [31].

Mobile urban air temperature monitoring via multiple methods overcomes these limitations by covering a larger geographic area than fixed-location sensor networks [32–34]. Other mobile methods, such as on-foot measurements of air temperature capture greater heterogeneity than fixed-location sensor networks, and neither air temperature measurements corresponded well to land surface measures [13]. Bike-based mobile monitoring has been shown to be an efficient, effective, and relatively inexpensive way to collect intra-urban temperatures across urban areas [15]. Mobile measurements have improved the ability to measure and model urban air temperature at human-relevant spatial scales and throughout the day, capturing relevant inter- and intra-day variation for heat monitoring [33–35].

Mobile air-temperature monitoring efforts demonstrate how the built environment and urban form influence urban heat. Early carbased air temperature research identified the cooling effects of urban open spaces in Utrecht in the Netherlands [32]. Bike-based research in Utrecht, The Netherlands found that the strongest predictors of the urban heat island were low sky view fraction (amount sky visible from the ground) and the high fractional building cover [15]. Based on car-collected data, the more urbanized and denser local climate zone types were 0.5 °C–2.0 °C degrees warmer than less urbanized zones in the French city Nancy [36]. Low density residential areas, with abundant vegetation were the coolest parts of Rotterdam, The Netherlands, based on a bike-collected data [29]. Three mid-Atlantic US cities were cooler in highly vegetated areas and/or with lower building density, while roadways were the hottest, especially when vegetation near roadways was minimal, based on car-mounted sensors and modeling [33]. Importantly the relationships between the built environment and heat varied throughout the day, making mobile observations critical for understanding diurnal urban heat trends [33,34].

Mobile sensors deployed at different times of day have captured inter- and intra-day variation relevant for heat monitoring. A pedestrian-based mobile monitoring system in Singapore showed that building shade can reduce temperature by as much as $4.5\,^{\circ}$ C, and vegetation can lower air temperatures up to $4\,^{\circ}$ C in the day time and $1.5\,^{\circ}$ C at night [37]. Although urban parks can be the coolest in the middle of the day, they can be as warm as industrial areas due to bodies of water that store and re-emit heat at night [29]. Patterns of shade change throughout the day [6] as well as with different cloud conditions, thus relationship between vegetation and surface temperature also reflect similar temporal non-stationarity [38]. How much and under what conditions landcover-air temperature relationships vary over time and across space remains poorly understood.

Some research has examined the non-stationarity among air temperature, tree canopy, and impervious surfaces over the course of a day using mobile monitoring [10,11]. Bike-based research in Madison, Wisconsin revealed that tree canopy cover ranging from 0 to 100 % cover within a 90 m buffer around bike locations were non-linearly associated with $\sim 1.5\,^{\circ}\text{C}$ lower air temperature in the afternoon ($\sim 16:00-18:00$ local time) [11]. Impervious surfaces were linearly associated with $1.3\,^{\circ}\text{C}$ warmer air temperatures [11]. Both cooling and warming effects were smaller in magnitude at night [11], again highlighting the importance of intra-day variation in landcover-heat relationships. Research in Washington, DC via car and using 200-m buffers showed that the difference in tree canopy cover from 5 % to 90 % was associated with $1.8\,^{\circ}\text{C}$ lower air temperature in the hottest part of the day (afternoon, 14:00-15:00 local time) and a slightly smaller $1.7\,^{\circ}\text{C}$ degree cooling effect in the evening (18:00-19:00) [10]. Concurrently, warming from impervious surfaces fell from $1.7\,^{\circ}\text{C}$ in the afternoon to $1.4\,^{\circ}\text{C}$ in the evening. Neither study accounted for cloud cover.

The lack of cloud measurement is especially important since trees reduce air temperatures via shading and evapotranspiration. Under cloudy conditions, the former effect is minimal and it is not well understood how much transpirational cooling persists under these conditions. Interestingly, it has been shown that cities even create clouds: they draw moisture in through advection and then a combination of turbulence from urban surface roughness and abundant urban aerosols create more clouds [16]. Excluding clouds

prevents us from understanding the role of trees' cooling under cloudy conditions. Further, the changing daily landcover-air temperature relationships might be different on hotter days rather than cooler. Ziter and colleagues[11] found more cooling from tree canopy cover on hotter days. To increase generalizability, more research in additional geographic locations is needed to better characterize and understand the relationships between landcover composition and air temperature across space and over time in conjunction with varied weather conditions.

This paper asks, 1) what are the relationships between air temperature and landcover, and how do they change throughout the day with varied cloud conditions? Because heat is a public health issue during especially hot periods, we also analyzed the land cover-air temperature relationships separately from the full dataset to understand whether the relationships changed. Next, we asked, 2) how do those landcover-air temperature relationships vary or not among the hottest 25th percentile days? We estimate how the relationships between landcover (tree canopy and impervious surface) and air temperature change throughout the day using bicycle-mounted air temperature sensors in New Haven, CT, from 2019 to 2021 and generalized additive mixed models (GAMM) across 156 rides. Land cover was summarized within 90-m buffers surrounding bike observations. The GAMMs used subsets of the data at different times of the day and controlled for cloud condition, wind speed and direction, elevation, and location, and ride. To evaluate the sensitivity to the time of day thresholds, the analyses were repeated with 1-h shifted subsets. The purpose of this paper is to understand how the relationship between land cover and air temperature change over time and across space, so that more realistic cooling benefits of urban trees can be obtained.

2. Methods

2.1. Study area

New Haven, Connecticut (population \sim 130,000), is a city located in southern New England north of the Long Island sound, USA (41°18′29.0"N, 72°55′38.3"W, Fig. 1A). The municipality is \sim 49.2 km², and the region is classified as Dfa in the Köppen-Geiger climate classification system, or Humid Continental Hot Summers With Year Around Precipitation [39]. The summers are warm and humid, the winters are cold and snowy, and it is partly cloudy all year. The mean annual temperature is 11.2 °C from 1981 to 2010, the mean annual January temperature is -1.11 °C, the mean annual July temperature is 23.33 °C, and the mean annual precipitation is 119.66 cm [40].

2.2. Bike-based measures

We took mobile measurements of air temperature data using sensors mounted on bicycles' handle bars. The "Smart-T" sensors communicate with cell phones to log GPS information for every temperature record (https://biking-for-science.yale.edu/sensors/smart-t; [41][42]). Sensors were contained within ABS-like resin radiation shields, and calibrated in a lab using two fans, which

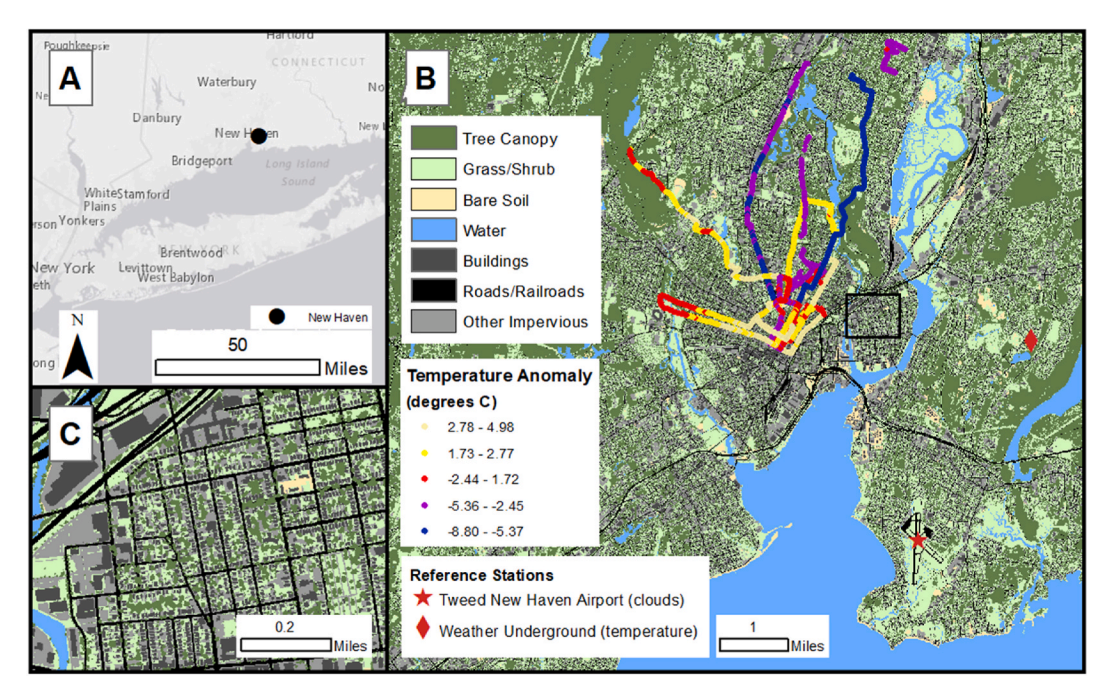


Fig. 1. New Haven in its regional context showing the Long Island Sound to the south (A), a sample of temperature-anomalous rides are overlaid on the high resolution (1 m^2), high-accuracy (\geq 95 %) landcover data (B), a close up of the detailed landcover data (C).

ensured that each sensor recorded ambient temperature accurately and consistently [42]. Each bike ride generates a data transect along a biking route by logging latitude, longitude, time, and temperature. The spatial resolution of such data transect is 4 m when biking at a speed of 4 m/s (i.e., 14.4 km/h). The sensor's response time to step changes in temperature is 9.7 (\pm 3.2) s.

We measured 156 transects. Rides occurred between June 15 and September 15 of each year between 2019 and 2021 to coincide with the warmest parts of the year. The biking routes start in highly impervious residential areas. Most routes were selected by volunteer cyclists (one coauthor, a university professor, and staff member) corresponding to their commuting routes. These volunteers took different routes to and from work and home to cover a larger area. This approach is both practical for data collection and may reflect common human experiences of urban heat but results in neither a fully random nor systematic sampling design (e.g. Fig. 1B). We therefore designed three additional routes to capture areas with high percent tree canopy cover, directing riders (incoming masters students) through one or more urban parks to ensure a range of land cover conditions were included. The routes were not the same each day, nor were the routes ridden at the same time, as a result the land cover summaries vary across hotter or cooler and/or cloudy days. The rides averaged 32 min, ranging from 1 to 86 (median 32, interquartile range = 19.11). Relatively short ride durations (i.e. ~30 min) were intended to reduce the influence of changing background temperature throughout a ride.

Parts of the tree canopy in each bike-based point comes from street trees. The street tree population varies in size and species; common species include oaks, maples, Honey locust, Bradford pear, ornamental cherry and apple trees, and dogwood [43]. The street inventory map can be found here: https://uri.yale.edu/maps/street-tree-inventory-map.

2.3. Temperature anomaly

The primary variable of interest was the bicycle-observed temperature minus the reference temperature (described next), hereafter "temperature anomaly". Temperature anomaly therefore represented how temperatures recorded by bicycle throughout the city differed from a spatially fixed-reference sensor.

We obtained reference temperature data from Weather Underground (WU; https://www.wunderground.com/). WU is an international network of individuals using weather stations to supply detailed, localized information. A station (KCTEASTH102; Fig. 1B) with complete data to match the bike rides was selected so that all bike-based observations could be included. KCTEASTH102 provides data in 5-min intervals, which were linearly interpolated to create 1 s timesteps so as to facilitate linkages with bike temperature data by date and time. KCTEASTH102 is in a suburban residential neighborhood and the landcover surrounding the station in a 90 m² buffer is 27 % tree canopy cover, 47 % grass/shrub, and 26 % impervious surfaces.

Because previous research has shown varying relationships throughout the day [10,11,34], we divided the data into five 3-h periods consisting of: morning (8:00–11:00), midday (11:00–14:00), afternoon (14:00–17:00), evening (17:00–20:00), and night (20:00–23:00, Table 1). Models were fit independently for each of the five subsets. In New Haven the sun sets at 19:01 on Sept 15, the shortest day of the year examined, and at 20:28 on June 21, the longest day. Therefore, sunsets mainly occurred within the evening chunk.

To address question #2 pertaining to the hottest observations, we retained only the upper quartile of hottest days based on ranking of the maximum temperature at the reference station on that day. The models per time of day were re-estimated with only those hottest 25 % of the data. To evaluate the sensitivity of chosen thresholds for the times of day as a robustness check (question #3), the analyses were performed again where each break was moved 1 h earlier, called the offset time analyses.

Table 1
Distribution of mobile air temperature sampling by time of day and year. All rides occurred between June 15 and September 15. Observations include temperature and time at a latitude/longitude point.

Time of Day	Year	Rides (n)	Observations (n)
Morning (8:00–11:00)	2019	19	21,291
morning	2020	15	17,878
morning	2021	1	257
morning	subtotal	35	39,426
midday (11:00-14:00)	2019	27	32,757
midday	2020	18	32,547
midday	2021	3	4090
midday	subtotal	48	69,394
Afternoon (14:00-17:00)	2019	6	6770
afternoon	2020	14	19,536
afternoon	2021	3	4425
afternoon	subtotal	23	30,731
evening (17:00-20:00)	2019	3	6085
evening	2020	21	28,541
evening	2021	1	930
evening	subtotal	25	35,556
night (20:00-23:00)	2020	22	23,550
night	2021	3	3222
night	subtotal	25	26,772
	Total	156	201,879

2.4. Predictor variables

The temperature anomaly response was modeled as a function of landcover (tree canopy and impervious surface) while controlling for key covariates (next section). High resolution ($\leq 1 \text{ m}^2$), high classification accuracy ($\geq 95 \%$) landcover mapping via object-based automated feature extraction techniques to a combination of high-resolution LiDAR and imagery (Fig. 1C) [44,45] resulted in a seven-class landcover dataset with a spatial resolution of 0.9144 m. This was followed by a comprehensive manual review in which errors observed at a scale of 1:3000 were corrected. Building, transportation (roads/railroads), and other impervious (e.g., sidewalks, parking lots, etc.) surfaces were combined to create a single, aggregated impervious surface class. Impervious surface and canopy area were extracted surrounding each of the 201,879 bike measurement locations at buffer distances of 10-, 30-, 60-, and 90-m for comparability with previous research [10,11]. The 10-, 30-, and 60-m analyses are shown in the appendix, since Ziter and colleagues (2019) found the best fit with 90 m buffers.

We accounted for other influences on air temperature including elevation, wind, and location. Elevation was derived from the same LiDAR used to create the landcover data. The digital elevation model value corresponding to each bike measurement point was extracted. Reference station data from KCTEASTH102 also included windspeed and direction over 16 bearings, which were reclassified into 8 cardinal directions (N, NE, W, SE, S, SW, W, NW) for ease of interpretation and model parsimony. Latitude and longitude were included to account for unexplained variance owing to geographic location and unmeasured covariates and to mitigate spatial autocorrelation (Ziter et al., 2019). Local Climatological Data were downloaded from NOAA's National Centers for Environmental Information (https://www.ncdc.noaa.gov/cdo-web/datasets/LCD/stations/WBAN:14758/detail) collected at the Tweed New Haven Airport to obtain cloud cover estimates (Fig. 1B).

2.5. Statistical analyses

Scatter plots of the entire dataset suggested nonlinearities between canopy and air temperature, and impervious surface and air temperature. Generalized Additive Mixed Models (GAMMs) estimate and weight a series of basis functions to flexibly fit smoothed, non-linear relationships between predictors and the dependent variable while penalizing to prevent overfitting [46]. GAMMs can be thought of as a balance between relatively inflexible and highly interpretable linear models, and machine learning techniques that are highly flexible but often difficult to interpret [47].

Each observation from a bicycle trip or "ride" bears resemblance to others on that same ride. Therefore, ride was included as a random intercept to account for the self-similarity contained within a ride at a relatively similar time of day and geographic area. The variety of rides across space and over time captured a diverse array of conditions, and the random intercept allows detection of unmeasured variability rather than assuming it away.

Because the data were spatially and temporally autocorrelated, traditional statistical assumptions of independence would not hold. However, given the large overall sample size, and large number of observations per each time strata, we employed a resampling approach. In the main analyses, for each of five times of day, we selected a 10 % subsample with replacement, fit a GAMM, then repeated this process 100 times. Each model therefore contained sufficient data relative to the number of estimated parameters, yet the probability of any draw being collected from nearby places, times, and/or ride was reduced. Predictions from each model run were then combined and used to derive mean and 95 % confidence intervals derived from each distribution of predictions at desired covariate values. The GAMMs used this formula:

$$temperature Anomaly_{x,y,t,r} = clouds Clear + wind Direction + s(tree Canopy Cover_{x,y,t,r}, by \ clouds Clear) + s(impervious Surface_{x,y,t,r}, by \ clouds Clear) + s(elevation_{x,y,t,r}) + s(wind Speed_{x,y,t,r}, by \ wind Direction_{x,y,t,r}) + s(lon, lat_{t,r}) + trip_r$$

$$(1)$$

Where $temperatureAnomaly_{x,y,t,r}$ is the bike-measured temperatures throughout the City of New Haven minus the reference station temperature at longitude x, latitude y, at time t, on ride r. The reference station was surrounded by grass in a suburban area. cloudsClear is a categorical variable with two values clear or not clear (comprised of the following conditions: few, scattered, or broken clouds, or overcast), windDirection is a categorical variable. s() is a smoother function with 3 knots for treeCanopyCover, tree

In order to understand the relationship between landcover (tree canopy cover and impervious surfaces) during the hottest days, the whole dataset was filtered to contain only the hottest 25 % of days based on the reference station's daily maxima. When analyzing on the hottest 25 % of the data, the subsample percentage was increased to 20 % to have enough data relative to the number of model parameters estimated. In the offset time analyses, the setup was the same except the time-of-day break was shifted 1 h earlier. The purpose was to understand the role of the chosen time of day thresholds.

To evaluate model fit by buffer size, the R^2 values were examined. Given the unexpected stability of R^2 values across buffer distances, the models were refit without the lon/lat smoother, which showed that larger buffer distances had higher R^2 values within a time of day, but the degree of those differences varied with time of day sensu Alonzo and colleagues [10] (not shown). For comparability with Ziter and colleagues [11], we focus on 90 m buffer models. The 10-, 30-, and 60-m results are shown in Figs. S1-S3.

Analyses were carried out using R version 4.1.2 (2021-11-01), data additional and details can be found in the reproducible code [48]. Because many of the routes originate or terminate at riders' homes, the first and last 200 points have been removed from each trip to preserve anonymity; the code will therefore not reproduce the exact same results. Fig. 1 was created with ArcMap version 10.8.2.

3. Results

The final dataset included 156 rides taken between June 15 and September 15 in years 2019, 2020, and 2021 (Table 1), representing a wide range of tree canopy and impervious cover percentages, cloudiness, elevation, and the reference station experienced a variety of wind speed and direction conditions, but wind mostly came from the South (Table 2, Table S1). Morning rides had notably less tree canopy cover (Table 2).

The models accounted for a substantial amount of variation in temperature anomaly. The R^2 values ranged from an average of 0.65 in the 10 m midday models, to a high of 0.96 in the 90 m afternoon models. Within a time of day, R^2 values did not vary substantively.

3.1. Changing land cover-air temperature relationships

The cooling benefits from tree canopy cover were strongest in the midday (11:00–14:00), afternoon (14:00–17:00), and morning (8:00–11:00) on clear days (Fig. 2). To summarize all of the estimates, the difference between model predictions at 100 % cover and 0 % cover are provided in Table S2. The difference in air temperature anomaly was -1.62 °C 95 % Confidence Interval (CI) [-1.63, -1.61], -1.19 °C [-1.21, -1.18], -1.15 °C [-1.18, -1.12], respectively, between 0 and 100 % tree canopy cover for midday, afternoon, and mornings. On cloudy rides in the morning and afternoon tree canopy was associated with temperature reductions above \sim 35–40 % canopy cover and the magnitude of the effect was comparatively small: -0.92 °C 95 % CI [-0.94, -0.89] and -0.51 °C 95 % CI [-0.53, -0.50], though morning rides tended to be along routes that had less tree canopy yielding greater uncertainty at high canopy fractions (Table 2, Fig. 2). Tree canopy in the midday and at night (20:00–23:00) under cloudy skies was associated with 0.53 °C 95 % CI [0.56, 0.50] and 1.43 °C 95 % CI [1.39, 1.46] warmer temperatures than the mostly grass-surrounded reference site, respectively, consistent with the idea that trees might be trapping heat in on cloudy nights when compared to open, grassy areas.

Relationships between impervious surface cover and temperature anomaly varied by cloud condition and time of day as well. For example, on clear mornings the relationship was concave, but convex on cloudy mornings, revealing important shifts in landcover-air temperature relationships. Warming from impervious surfaces was most pronounced in the evening (17:00–20:00) 1.11 °C 95 % CI [1.11, 1.11] on clear and cloudy rides, and during cloudy nights (20:00–23:00) and cloudy mornings 1.03 °C 95 % CI [1.03, 1.04] when impervious cover ranged from 0 to 100 %. Such observations are consistent with the idea that impervious surfaces effectively extend the period of time when human health is at greatest risk by elongating the period of exposure to high air temperatures.

3.2. Sensitivity analyses

Offset time analyses added more support for temporal non-stationarity in the relationship between landcover around bike trips and air temperature. Each time-of-day break was shifted 1 h earlier (descriptive statistics, Table S3), and several estimates changed substantially (Fig. 3). For tree canopy, shifting the definition of morning by 1 h resulted in a change from a nonlinear cooling when cloudy and roughly linear cooling when clear at high percent tree canopy cover, to no mean cooling and high uncertainty for both cloudy and non-cloudy conditions. These shifts are plausibly due to the combination of lower sample size, less tree canopy cover in those observations, and that the sun had not yet warmed the study area, which could be addressed with future research. In the midday cloudy rides, the relationship shifted from a strongly non-linear, concave warming 0.53 °C [0.5, 0.56] to an approximately linear (median effective degrees of freedom = 1.02) cooling effect -0.28 °C [-0.30, -0.25]. Consistent with the main findings, there were significant cooling effects during the clear midday period -1.43 °C [-1.43, -1.42], on cloudy afternoons -1.17 °C [-1.19, -1.16], and on clear afternoons -1.12 °C [-1.13, -1.10]. Clear evenings -1.09 °C [-1.15, -1.03] also showed a significant cooling effect. Compared to the main analyses (Fig. 2), the clear and cloudy estimates for impervious surfaces in mornings become similar, while the midday relationships become dissimilar in the offset time analyses (Fig. 3). The warming effects of impervious surface cover grew stronger and more linear at night.

Table 2
Summary of temperature anomaly, landcover, elevation and wind speed. Median (IQR).

Characteristic	Overall, $N = 201,879$	Morning $N = 39,426$	$\begin{array}{l} \text{midday} \\ \text{N} = 69,\!394 \end{array}$	$\begin{array}{l} Afternoon \\ N=30{,}731 \end{array}$	Evening N = 35,556	$\begin{array}{l} \text{night,} \\ N=26{,}772 \end{array}$
Temperature Anomaly	0.64 (-0.20, 1.41)	0.86 (0.19, 1.50)	0.62 (-0.09, 1.28)	-0.33 (-2.06, 0.60)	0.35 (-0.57, 1.19)	1.75 (0.95, 2.41)
Tree Cover (%, 90 m)	23 (13, 36)	15 (13, 29)	24 (13, 37)	25 (14, 46)	24 (14, 39)	22 (14, 33)
Impervious Surface (%, 90 m)	53 (32, 67)	55 (46, 67)	47 (30, 63)	50 (25, 64)	56 (29, 71)	58 (40, 71)
Elevation (m)	41 (27, 60)	44 (28, 61)	42 (26, 60)	42 (28, 99)	41 (28, 46)	37 (26, 44)
Wind Speed (miles per hour)	0.85 (0.16, 1.77)	1.21 (0.50, 1.77)	1.24 (0.68, 2.28)	0.60 (0.25, 1.10)	0.27 (0.00, 0.96)	0.00 (0.00, 1.40)

Predicted temperature anomaly:

90 meter buffer

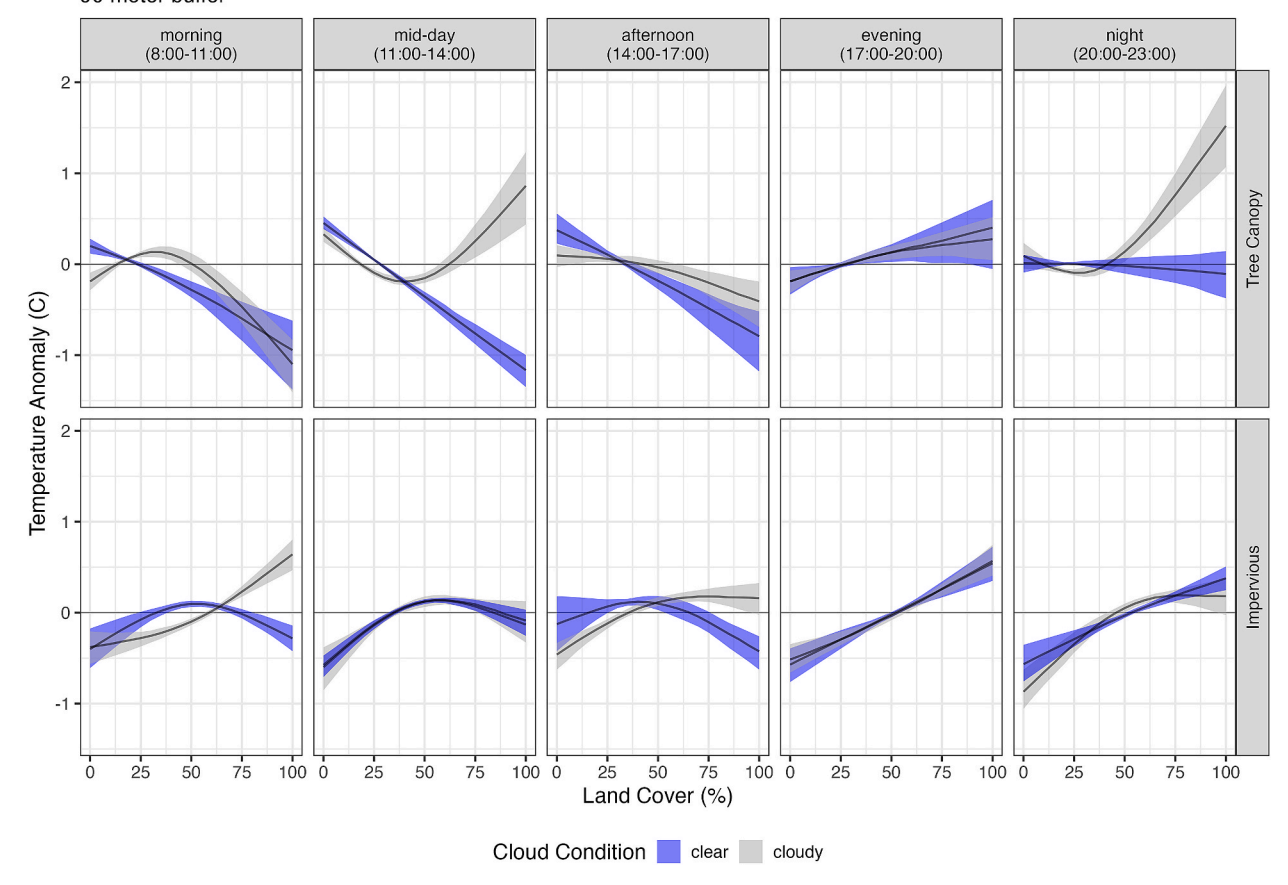


Fig. 2. Estimated temperature anomaly (bike temperature minus reference station) from tree canopy (top) and impervious surface (bottom) in 90 m buffers by cloud condition from resampled generalized additive mixed models controlling for elevation, location, trip, and wind speed per direction.

3.3. Hottest-day analyses

Filtering for the hottest 25 % of days based on the reference site's daily maxima, the resulting reference observations were 29–33 °C and contained no nighttime temperatures. Among the hottest days, tree canopy was associated with lower temperatures on clear afternoons -1.78 °C 95 % CI [-1.78, -1.78], cloudy midday -1.17 °C 95 % CI [-1.19, -1.15], clear midday -1.12 °C 95 % CI [-1.12, -1.11] (Fig. 4, Table S2). Concurrently, the warming effect of impervious surfaces was strongest on clear and cloudy afternoons up to \sim 50 % cover, and during clear evenings 2.07 °C 95 % CI [2.05, 2.09]. Counterintuitively, tree canopy was associated with greater temperature anomalies on hot, cloudy afternoons above \sim 30 % tree canopy, on hot, clear evenings below 30 % cover. It is possible that earlier in the day there were clear conditions for those particular observations, and residual warming from the sun affects these estimates. Additionally, greater impervious surface cover on clear evenings was associated with a linear cooling effect of -1.55 °C 95 % CI [-1.59, -1.52]. This could be due to spatial miss-matches between bike observations and the temperature reference station; the reference may have been beneath cloudy skies. Nonetheless, it seems clear that under local conditions, relationships between landcover and temperature anomaly change throughout the day and are in some cases different from the larger, all-encompassing dataset.

4. Discussion

4.1. Trees cool, impervious surface warms, and those relationships change throughout the day with cloud cover

We found that the relationship between landcover and cooling or warming changes throughout the day, as described by prior research [10,11]. We identified stronger cooling benefits in the midday, afternoon, and during the morning on clear days. Similar to prior research, we also found a $1.62\,^{\circ}$ C cooling effect on clear days between 11:00 and 14:00, and $1.19\,^{\circ}$ C effect between 14:00 and 17:00. On the hottest clear days (top $25\,^{\circ}$ M hottest of reference station's daily maxima) tree canopy cooled $1.12\,^{\circ}$ C from 11:00 to 14:00 and $1.78\,^{\circ}$ C from 14:00-17:00. In Washington, D.C. the cooling effect was $\sim 1.8\,^{\circ}$ C from 14:00-15:00 local time [10] and in Madison,

Predicted temperature anomaly:

90 meter buffer (shifted sensitivity analysis)

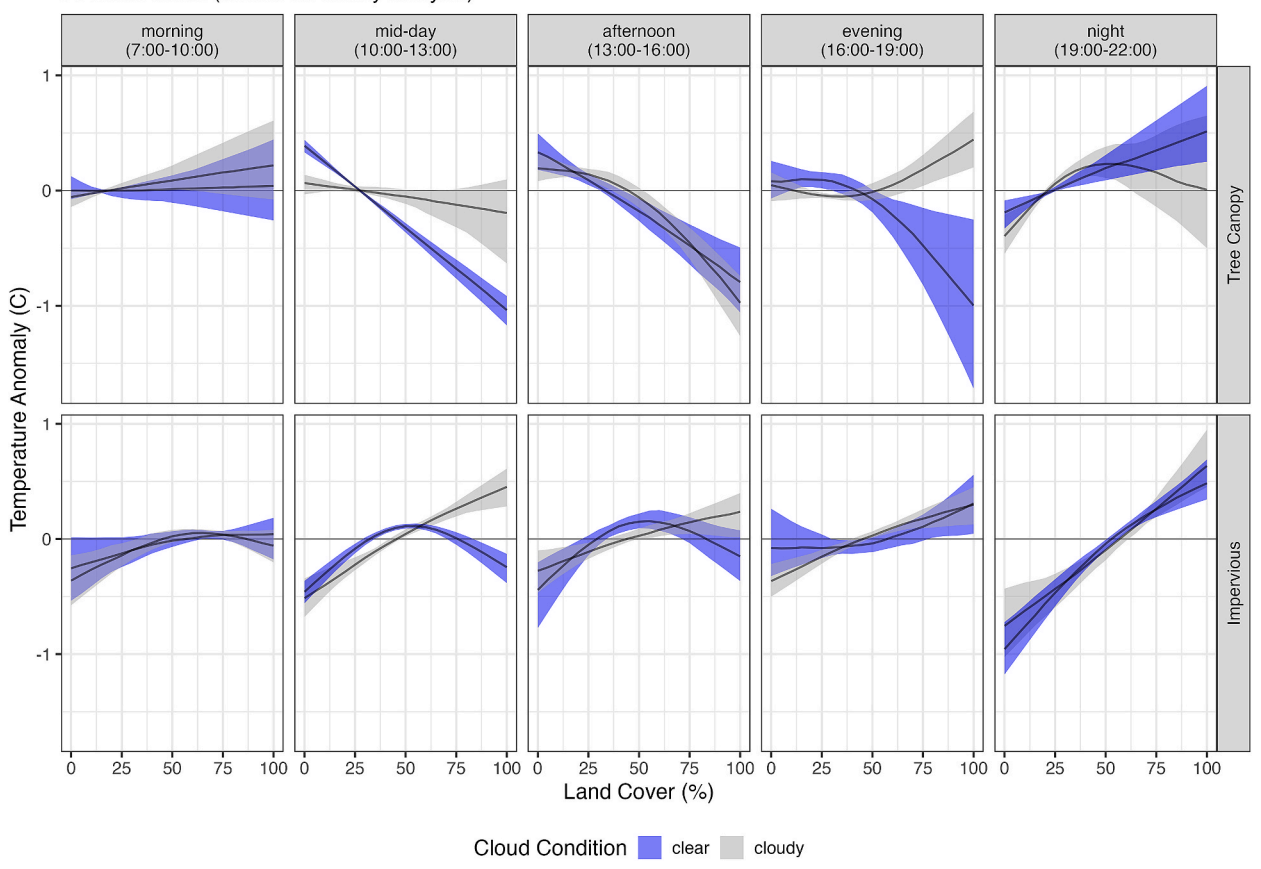


Fig. 3. Results of the offset time analyses where the time breaks were shifted an hour earlier. Note the different vertical axes lengths to accommodate larger estimates and uncertainty.

Wisconsin the cooling effect was \sim 1.5 °C from 16:00–18:00 local time [11]. However, our paper uses measurements spread more continuously through the day to highlight changing diurnal variation. It is possible that the many rides used here, spanning months and years, better capture the range of how changing meteorological conditions may alter the landcover-air temperature relationships over a day, and offer greater generalizability.

The shapes of the prediction curves bear some similarities and some key differences to prior related research, while highlighting the importance of including cloud condition. Prior research in Madison, Wisconsin [11] identified a threshold of tree canopy cover ~35–40 % within a 90 m buffer, with minimal cooling below that level. Research in Washington, D.C. found a roughly linear cooling effect that was stronger in the afternoon and evenings than during the predawn hours [10]. Those later findings match our clear-day relatively linear morning, midday, and afternoon findings. This could be due to the smaller geographic study area, less sampling in large, forested parks, and a larger overall apparent role of transpirational cooling rather than shading. However, our cloudy models suggest tree canopy-related warming in the midday and at night. Moreover, key landcover-air temperature relationships varied with cloud condition. For example, morning tree canopy and air temperature relations were concave when clear, and convex when cloudy. This pattern would have gone unobserved without explicitly including cloud cover in the analysis. Satellite-based land cover analyses are incapable of detecting such dynamics. It has been suggested that aerodynamic roughness of trees can trap heat in cities [7], and that cities have more cloud cover than their rural surroundings due to the combination of cities advected moisture in, surface roughness creates turbulence, and abundant urban aerosols [16]. If cities do indeed create clouds, the sum total of these complex and interacting mechanisms may mean that tree canopy cover on cloudy days can be associated with greater temperatures, which were observed here (Fig. 2).

Urban trees reduce temperatures via evapotranspiration and shading. The role of shading was reduced under cloudy conditions, specifically in the afternoon, when our main results showed significant cooling on clear (-1.19 °C) and cloudy (-0.51 °C) rides, whereas the offset time analyses also showed similarly significant cooling on clear (-1.12 °C) and cloudy (-1.17 °C) rides. More muted, but still significant, reductions in temperature anomalies under cloudy conditions reinforce the importance of evapotranspirative cooling for air temperature. The role of shading was also diminished in midday models when the sun is typically at its zenith and air temperature is warming to due convection following a morning of surface heating. Nevertheless, on clear days tree

Predicted temperature anomaly:

90 meter buffer (hottest 25% days)

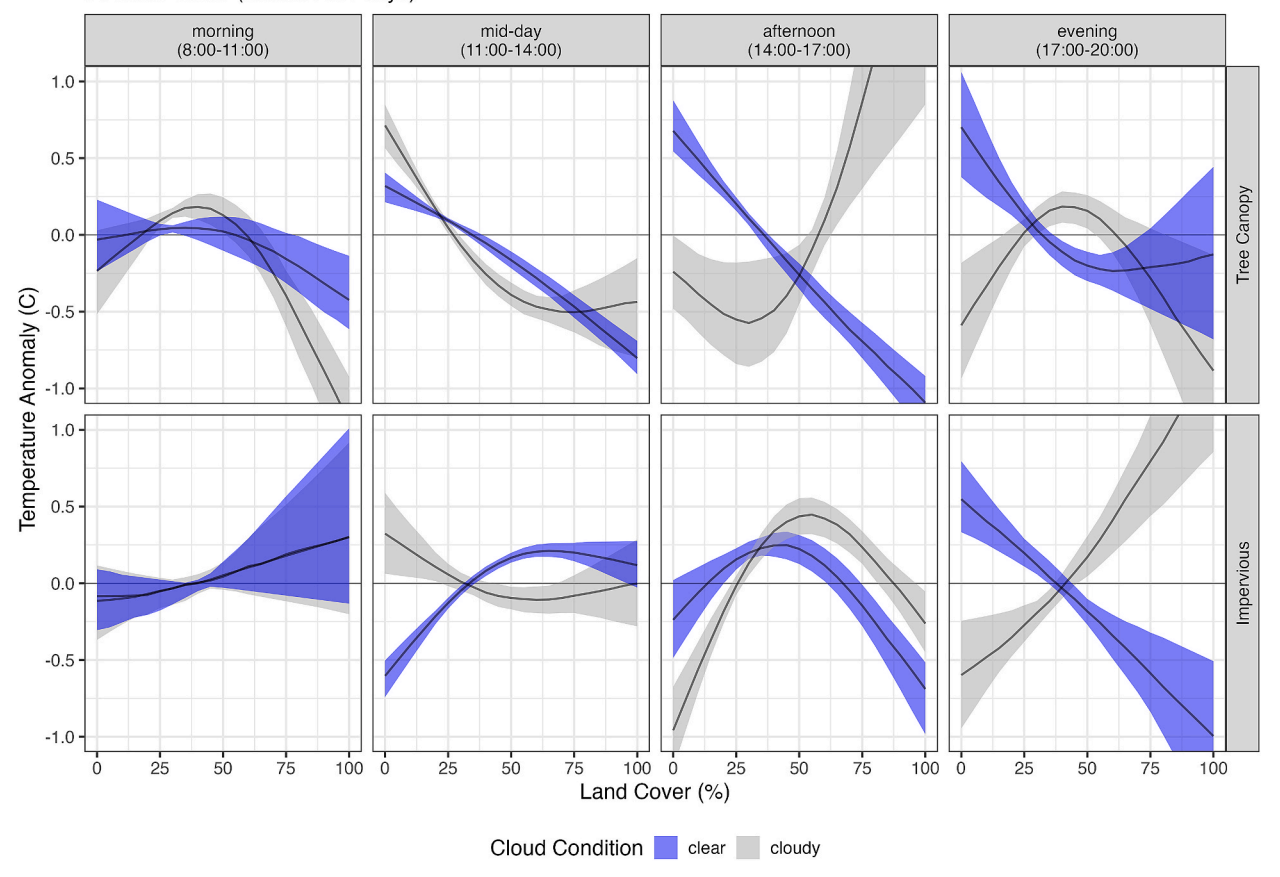


Fig. 4. Estimated temperature anomaly (bike temperature minus reference station) on the hottest 25 % of the reference station's daily maxima, which were 29–33 °C.

canopy reduced temperatures by $1.62\,^{\circ}$ C in the main analyses, $1.43\,^{\circ}$ C in the offset time analyses, and $1.12\,^{\circ}$ C on the hottest days in the midday time period. Sampling campaigns designed to measure the hottest days may therefore underestimate the cooling benefits of urban trees, though more research is needed.

Higher impervious surface fractional cover was almost always associated with higher temperatures in our models, except at extremely high levels of cover (90–100 %) during the midday and afternoon periods. This could be due to taller buildings casting longer shadows in the downtown area creating a canyon effect, where such levels of impervious cover were likely to occur. Buildings shade has been shown to reduce air temperature by as much as 4.5 °C in Singapore [37].

We studied land cover-air temperature relationships changing over the course of a day and note that surface temperature studies cannot directly explain the role of clouds when relying on remotely sensed imagery. The sampling here represents large mobile sampling campaign (>200,000 observations) specifically to test the relationships between air temperature and landcover. Road-based sampling with cars and/or bikes are spatially-biased to road networks and sidewalks, which are composed of impervious surfaces and may bias results relative to the entire mix of urban land uses and landcovers [33,35]. A strength of this study is the use of volunteers on their commuting routes focuses analyses on corridors in heavy use by residents and may better reflect common experiences than randomly chosen paths.

4.2. Limitations and directions for future research

The analyses here added landcover (tree canopy and impervious surface) to the study of urban microclimates that have tended to focus on vegetation in general [37], greenspaces like parks [29,49], pavement types [8,50,51], types of shade [12], building type and configuration [13,14], land use [15], and other elements of urban form [32,34,36,37]. Our focus on tree canopy and impervious surface did not include these other important factors. Future research might consider deliberately adding more routes to achieve more landcover end members (100 % tree canopy or impervious surface cover), and over a wider range of times per day. Moreover, sampling could occur within parks or urban forest patches on foot [37], or be included on bus routes to designed to cover large spatial extents with higher frequency [35]. Debates on creating the optimal sampling network, the utility, accuracy, and cost effectiveness of fixed

versus mobile versus hybrid sensor networks notwithstanding [35,52,53], future mobile sampling campaigns represent an exciting opportunity for public science and engagement, as well [54]. Additional, multi-modal (on foot, by bike, on scooters, with busses, etc) mobile monitoring with a greater spatial extent, including more sources of environmental variation over a greater range of meteorological conditions, and carried out by community members in a fun and educational manner represents an important environmental science research-educational opportunity.

More sophisticated measures of canopy spatial arrangement such as patch size and shape have been shown to be important for urban surface temperature via tree canopy cover [25]. How do several small patches of canopy cool air relative to a larger patch of the same total size? Large urban parks in Addis Ababa, Ethiopia have substantially lower surface temperature [49] and air temperatures were considerably lower in parks in Rotterdam, The Netherlands [29] than the surrounding urban matrix. However, unique high-resolution land surface temperature research showed that small patches of vegetation in residential yards provided disproportionate cooling benefits during an extreme heat waves in Adelaide, Australia [55]. Configuration and adjacency of urban vegetation could also be included in future studies [26]. Ultimately, we may better understand the urban heat island by separating out tree canopy hanging over various surfaces including woodland soils, roofs, or pavement [10], by including different types of impervious surfaces [50,51], and considering size, shape, configuration [26], and adjacency of different landcover types.

A notable difference between this research and prior related work pertains to the landcover maps. Both Ziter and colleagues [11] and Alonzo and colleagues [10] had tree and impervious surfaces as non-exclusive classes; tree canopy over impervious surface was classified as impervious and again as tree canopy. In fact, Alonzo et al. (2021) demonstrated the importance of distinguishing these classes explicitly. Here tree canopy and impervious surfaces were mutually exclusive categories. Trees overhanging impervious surfaces were assigned to the tree category. Since these two landcover classes were part of the same whole, they were more strongly correlated – to an extent – by construction (10 m buffer r=-0.814, 90 m buffer r=-0.839, p<0.0001). Moreover, Madison, Wisconsin had substantially more grass/shrub area, which lowered the tree canopy/impervious correlation. We did not include an interaction between canopy and impervious (like both Ziter and Alonzo) due to their high bivariate correlation (from construction and actual landscape conditions), high collinearity, and high concurvity. Future landcover-air temperature analyses in a greater set of locations could make use of the Chesapeake Conservancy's (2022) freely available high-resolution (1 m^2) high-accuracy [56] 12-class landcover dataset for the entire Chesapeake Bay watershed, covering ~200 counties and jurisdictions (https://chesapeakeconservancy.org/conservation-innovation-center-2/high-resolution-data/land-cover-data-project/). The 12 classes include tree canopy, tree canopy over structures, tree canopy over impervious surfaces, and tree canopy over impervious roads. Therefore, tree canopy and impervious surfaces are not part of the same whole, and they better reflect class differences in 3-dimensional space.

Different types of pavements have different relationships with air temperature, too [50]. It has also been suggested that different subclasses of impervious surface (e.g., roads vs buildings vs parking lots) could be analyzed separately [20], and may have different relationships with air temperature [34], which the Chesapeake Conservancy layer also supports. Tree canopy cools via shading and transpiration mechanisms, evaluating tree canopy over different surfaces may provide clues about the unique – and additive – benefits of those two different mechanisms.

Temporally-lagged predictors might be useful in future research. For example, a cloudy afternoon might have been preceded by a sunny morning. That would lead to different estimates than a cloudy morning with a subsequently clear afternoon. In both cases, only looking at the afternoon conditions may have missed the role of cloud cover in the prior time period.

Future research could incorporate the benefits of larger spatial extents and repeated measures from mobile sensors, with mean radiance, which may better reflect the lived experience with respect to heat stress and human perceptions of heat [8,12]. Mean radiance factors in the thermal burden on a person even better than air temperature. A hand-pulled wagon or 'MaRTy' cart [57], equipped with temperature, humidity, radiance sensors, cameras, and other sensors mounted in multiple directions have shown the importance of different types of shade from buildings, trees, and different types of shade structures, etc. [12], and reflective pavements [8,50] for urban cooling or warming. Additional mobile mean radiance measures represent an important research frontier.

5. Conclusions

Our findings support the interpretation that the relationship between landcover and air temperature changes based on time of day, cloud cover conditions, and extreme heat. We found the strongest cooling benefits of tree canopy in the clear morning, midday, and afternoon conditions, and not during the evening or at night. The cooling effect was comparatively smaller on cloudy mornings and afternoons. The cooling benefits of tree canopy were close to linear in most cases, even though some other similar studies have indicated a non-linear, threshold-like effect. The cooling was more muted at night (perhaps due to trapping heat in), under cloudy conditions, and during the hottest observations. Warming from impervious surfaces was most pronounced in the evening irrespective of clouds, and during cloudy nights and cloudy mornings. We add a broader spectrum of weather conditions by explicitly including clouds, and greater temporal resolution by measuring throughout the day to bike-based urban heat research. Future mobile sampling campaigns may broaden the spatial extent with more environmental variation, representing an opportunity for public science and engagement, and contribute to more reasonable expectations about the benefits realized through maintaining and expanding urban tree canopy cover.

Data availability statement

Data and reproducible code are available via [48]. Because many of the routes originate or terminate at riders' homes, the first and

last 200 points have been removed from each trip to preserve anonymity; the code will therefore not reproduce the exact same results.

Funding

The Urban Resources Initiative provided funding for this project

CRediT authorship contribution statement

Dexter Henry Locke: Writing – review & editing, Writing – original draft, Software, Project administration, Methodology, Formal analysis, Data curation, Conceptualization. **Matthew Baker:** Writing – review & editing, Supervision, Methodology, Investigation, Conceptualization. **Michael Alonzo:** Writing – review & editing, Supervision, Methodology, Investigation, Conceptualization. **Yichen Yang:** Writing – review & editing, Methodology, Formal analysis, Data curation. **Carly D. Ziter:** Writing – review & editing, Project administration, Methodology, Investigation, Conceptualization. **Colleen Murphy-Dunning:** Writing – review & editing, Validation, Supervision, Project administration, Conceptualization. **Jarlath P.M. O'Neil-Dunne:** Writing – review & editing, Methodology, Data curation, Conceptualization.

Declaration of competing interest

The authors declare that they have no known competing financial interests or personal relationships that could have appeared to influence the work reported in this paper.

Acknowledgements

Thanks to all of the bike riders: Sara Smiley Smith, Mark Bradford, Alishia, Allison, Alison, Bridget, Cameron, Elizabeth, Ella, Jenna, Jonathan, Julian, Klara, Krista, Marrisa, Neil, Rudyan, Sally, Sandy, and Urvi. Ruth Engel (UCLA) provided helpful comments which strengthened the paper. Quentin Read provided code for paralyzing the resampling models, which greatly improved speed and performance, for which the authors are extremely grateful. The findings and conclusions in this publication are those of the author(s) and should not be construed to represent any official USDA or U.S. Government determination or policy.

Appendix A. Supplementary data

Supplementary data to this article can be found online at https://doi.org/10.1016/j.heliyon.2024.e25041.

References

- [1] R.F. Young, Planting the living city, J. Am. Plann. Assoc. 77 (2011) 368-381, https://doi.org/10.1080/01944363.2011.616996.
- [2] L.L. Kimball, P.E. Wiseman, S.D. Day, J.F. Munsell, Use of urban tree canopy assessments by localities in the Chesapeake Bay watershed, Cities Environ 7 (2014)

 9. http://digitalcommons.lmu.edu/cate/vol7/iss2/9.
- [3] P.R. Epstien, E. Mills, K. Frith, E. Linden, B. Thomas, R. Weireter, Climate Change Futures: Health, Ecological and Economic Dimensions, Boston, MA, 2005.
- [4] G. Luber, M. McGeehin, Climate change and extreme heat events, Am. J. Prev. Med. (2008), https://doi.org/10.1016/j.amepre.2008.08.021.
- [5] G.A. Meehl, C. Tebaldi, More intense, more frequent, and longer lasting heat waves in the 21st century, Science 305 (80) (2004) 994–997, https://doi.org/
- [6] Q. Yu, W. Ji, R. Pu, S. Landry, M. Acheampong, J. O'Neil-Dunne, Z. Ren, S. Tanim, A preliminary exploration of the cooling effect of tree shade in urban landscapes, Int. J. Appl. Earth Obs. Geoinf. 92 (2020) 102161, https://doi.org/10.1016/j.jag.2020.102161.
- [7] N. Meill, G. Manoli, P. Burlando, J. Carmeliet, W.T.L. Chow, A.M. Coutts, M. Roth, E. Velasco, E.R. Vivoni, S. Fatichi, Tree effects on urban microclimate: diurnal, seasonal, and climatic temperature differences explained by separating radiation, evapotranspiration, and roughness effects, Urban For. Urban Green. 58 (2021) 126970, https://doi.org/10.1016/j.ufug.2020.126970.
- [8] V.K. Turner, M.L. Rogers, Y. Zhang, A. Middel, F.A. Schneider, J.P. Ocón, M. Seeley, J. Dialesandro, More than surface temperature: mitigating thermal exposure in hyper-local land system, J. Land Use Sci. 17 (2022) 79–99, https://doi.org/10.1080/1747423X.2021.2015003.
- [9] A. Paschalis, T. Chakraborty, S. Fatichi, N. Meili, G. Manoli, Urban forests as main regulator of the evaporative cooling effect in cities, AGU Adv 2 (2021), https://doi.org/10.1029/2020av000303.
- [10] M. Alonzo, M.E. Baker, Y. Gao, V. Shandas, Spatial configuration and time of day impact the magnitude of urban tree canopy cooling, Environ. Res. Lett. 16 (2021) 84028, https://doi.org/10.1088/1748-9326/ac12f2.
- [11] C.D. Ziter, E.J. Pedersen, C.J. Kucharik, M.G. Turner, Scale-dependent interactions between tree canopy cover and impervious surfaces reduce daytime urban heat during summer, Proc. Natl. Acad. Sci. USA 116 (2019) 7575–7580, https://doi.org/10.1073/pnas.1817561116.
- [12] A. Middel, S. AlKhaled, F.A. Schneider, B. Hagen, P. Coseo, 50 Grades of shade, Bull. Am. Meteorol. Soc. (2021) 1–35, https://doi.org/10.1175/bams-d-20-0193.1.
- [13] P.K. Tsin, A. Knudby, E.S. Krayenhoff, H.C. Ho, M. Brauer, S.B. Henderson, Microscale mobile monitoring of urban air temperature, Urban Clim. 18 (2016) 58–72, https://doi.org/10.1016/j.uclim.2016.10.001.
- [14] M. Takata, Evaluating the influence of traditional land allotment in the historical district of Japanese regional urban center upon outdoor summer thermal environment, Japan Archit. Rev. 3 (2020) 33–43, https://doi.org/10.1002/2475-8876.12134.
- [15] T. Brandsma, D. Wolters, Measurement and statistical modeling of the urban heat island of the city of Utrecht (Netherlands), J. Appl. Meteorol. Climatol. 51 (2012) 1046–1060, https://doi.org/10.1175/JAMC-D-11-0206.1.
- [16] T.T. Vo, L. Hu, L. Xue, Q. Li, S. Chen, Urban effects on local cloud patterns, Proc. Natl. Acad. Sci. USA 120 (2023) 1–11, https://doi.org/10.1073/pnas.2216765120.
- [17] T.R. Oke, City size and the urban heat island, Atmos. Environ. (1973) 769-779.

- [18] T.R. Oke, The energetic basis of the urban heat island, O. J. R. Meteorol. Soc. 108 (1982) 1-24, https://doi.org/10.1002/qj.49710845502.
- [19] W. Zhou, G. Huang, S.T. Pickett, J. Wang, M.L. Cadenasso, T. McPhearson, J.M. Grove, J. Wang, Urban tree canopy has greater cooling effects in socially vulnerable communities in the US, One Earth 4 (2021) 1764–1775, https://doi.org/10.1016/j.oneear.2021.11.010.
- [20] J. Lin, H. Zhang, M. Chen, Q. Wang, Socioeconomic disparities in cooling and warming efficiencies of urban vegetation and impervious surfaces, Sustain. Cities Soc. 92 (2023) 104464, https://doi.org/10.1016/j.scs.2023.104464.
- [21] A. Ornelas, A. Cordeiro, J.M. Lameiras, Thermal comfort assessment in urban green spaces: contribution of thermography to the study of thermal variation between tree canopies and air temperature, Land 12 (2023), https://doi.org/10.3390/land12081568.
- [22] H. Pearsall, Staying cool in the compact city: vacant land and urban heating in Philadelphia, Pennsylvania, Appl. Geogr. 79 (2017) 84–92, https://doi.org/10.1016/j.apgeog.2016.12.010.
- [23] A. Elmes, J. Rogan, C. Williams, S. Ratick, D. Nowak, D.G. Martin, Effects of urban tree canopy loss on land surface temperature magnitude and timing, ISPRS J. Photogrammetry Remote Sens. 128 (2017) 1–52, https://doi.org/10.1016/j.isprsjprs.2017.04.011.
- [24] A.A. Scott, B. Zaitchik, D.W. Waugh, K. O'Meara, Intraurban temperature variability in Baltimore, J. Appl. Meteorol. Climatol. 56 (2017) 159–171, https://doi.org/10.1175/JAMC-D-16-0232.1.
- [25] C.S. Greene, P.J. Kedron, Beyond fractional coverage: a multilevel approach to analyzing the impact of urban tree canopy structure on surface urban heat islands, Appl. Geogr. 95 (2018) 45–53, https://doi.org/10.1016/j.apgeog.2018.04.004.
- [26] J. Yan, W. Zhou, G.D. Jenerette, Testing an energy exchange and microclimate cooling hypothesis for the effect of vegetation configuration on urban heat, Agric. For. Meteorol. 279 (2019) 107666, https://doi.org/10.1016/j.agrformet.2019.107666.
- [27] T. Chakraborty, A. Newman, Y. Qian, A. Hsu, G. Sheriff, Residential segregation and urban heat stress disparities in the United States, One Earth 6 (2022) 738–750, https://doi.org/10.1016/j.oneear.2023.05.016.
- [28] J. Cao, W. Zhou, W. Yu, X. Hu, M. Yu, J. Wang, Urban Climate Urban expansion weakens the contribution of local land cover to urban warming, Urban Clim. 45 (2022) 101285, https://doi.org/10.1016/j.uclim.2022.101285.
- [29] B.G. Heusinkveld, G.J. Steeneveld, L.W.A. Van Hove, C.M.J. Jacobs, A.A.M. Holtslag, Spatial variability of the rotterdam urban heat island as influenced by urban land use, J. Geophys. Res. 119 (2014) 677–692, https://doi.org/10.1002/2012JD019399.
- [30] L.G. Ioannou, K. Mantzios, L. Tsoutsoubi, S.R. Notley, P.C. Dinas, M. Brearley, Y. Epstein, G. Havenith, M.N. Sawka, P. Bröde, I.B. Mekjavic, G.P. Kenny, T. E. Bernard, L. Nybo, A.D. Flouris, Indicators to assess physiological heat strain—Part 1: systematic review, Temperature 9 (2022) 227–262, https://doi.org/10.1080/23328940.2022.2037376.
- [31] B.F. Zaitchik, C. Tuholske, Earth observations of extreme heat events: leveraging current capabilities to enhance heat research and action, Environ. Res. Lett. 16 (2021), https://doi.org/10.1088/1748-9326/ac30c0.
- [32] L.A. Conrads, J.C.H. Van Der Hage, A new method of air-temperature measurement in urban climatological studies, Atmos, Environ. Times 5 (1971) 629–635, https://doi.org/10.1016/0004-6981(71)90119-3.
- [33] V. Shandas, J. Voelkel, J. Williams, J. Hoffman, Integrating satellite and ground measurements for predicting locations of extreme urban heat, Climate 7 (2019) 1–13, https://doi.org/10.3390/cli7010005.
- [34] J. Voelkel, V. Shandas, Towards systematic prediction of urban heat islands: grounding measurements, assessing modeling techniques, Climate 5 (2017), https://doi.org/10.3390/cli5020041.
- [35] R. Shi, B.F. Hobbs, B.F. Zaitchik, D.W. Waugh, A.A. Scott, Y. Zhang, Monitoring intra-urban temperature with dense sensor networks: fixed or mobile? An empirical study in Baltimore, MD, Urban Clim. 39 (2021) 100979, https://doi.org/10.1016/j.uclim.2021.100979.
- [36] F. Leconte, J. Bouyer, R. Claverie, M. Pétrissans, Using Local Climate Zone scheme for UHI assessment: evaluation of the method using mobile measurements, Build. Environ. 83 (2015) 39–49, https://doi.org/10.1016/j.buildenv.2014.05.005.
- [37] M. Chàfer, C.L. Tan, R.J. Cureau, W.N. Hien, A.L. Pisello, L.F. Cabeza, Mobile measurements of microclimatic variables through the central area of Singapore: an analysis from the pedestrian perspective, Sustain. Cities Soc. 83 (2022), https://doi.org/10.1016/j.scs.2022.103986.
- [38] Y. Yin, L. He, P.O. Wennberg, C. Frankenberg, Unequal Exposure to Heatwaves in Los Angeles: Impact of Uneven Green Spaces, 2023, pp. 1–9, https://doi.org/10.1126/sciadv.ade8501, 8501.
- [39] M. Kottek, J. Grieser, C. Beck, B. Rudolf, F. Rubel, World map of the Köppen-Geiger climate classification updated, Meteorol. Z. 15 (2006) 259–263, https://doi.org/10.1127/0941-2948/2006/0130.
- [40] NOAA, Data Tools: 1981-2010 Normals, 2020. www.ncdc.noaa.gov/cdo-web/datatools/normals.
- [41] C. Cao, Y. Yang, Y. Lu, N. Schultze, P. Gu, Q. Zhou, J. Xu, X. Lee, Performance evaluation of a smart mobile air temperature and humidity sensor for characterizing intracity thermal environment, J. Atmos. Ocean. Technol. 37 (2020) 1891–1905, https://doi.org/10.1175/JTECH-D-20-0012.1.
- [42] Y. Yang, Evaluating the Role of Microclimate Change in Urban Heat Island Using Mobile Measurement, 2020. https://environment.yale.edu/mods.
- [43] B. Troxel, M. Piana, M.P. Ashton, C. Murphy-Dunning, Relationships between bole and crown size for young urban trees in the northeastern USA, Urban For. Urban Green. 12 (2013) 144–153, https://doi.org/10.1016/j.ufug.2013.02.006.
- [44] S.W. MacFaden, J.P.M. O'Neil-Dunne, A.R. Royar, J.W.T.T. Lu, A.G. Rundle, High-resolution tree canopy mapping for New York City using LIDAR and object-based image analysis, J. Appl. Remote Sens. 6 (2012), https://doi.org/10.1117/1.JRS.6.063567.
- [45] J.P.M. O'Neil-Dunne, S.W. MacFaden, A.R. Royar, K.C. Pelletier, An object-based system for LiDAR data fusion and feature extraction, Geocarto Int. 28 (2013) 227–242, https://doi.org/10.1080/10106049.2012.689015.
- [46] E.J. Pedersen, D.L. Miller, G.L. Simpson, N. Ross, Hierarchical generalized additive models in ecology: an introduction with mgcv, PeerJ 7 (2019) e6876, https://doi.org/10.7717/peerj.6876.
- [47] A.F. Zuur, E.N. Ieno, N.J. Walker, A.A. Saveliev, G.M. Smith, Mixed Effects Models and Extenstions in Ecology with R, Springer, 2009, https://doi.org/10.1017/CR09781107415324 004
- [48] D.H. Locke, M.E. Baker, M. Alonzo, Y. Yang, C.D. Ziter, C. Murphy-Dunning, J.P. O'Neil-Dunne, Data and Replication Code for Analyzing the Variation in Urban Tree Canopy and Air Temperature Reduction in New Haven, CT, 2024, pp. 2019–2021, https://doi.org/10.2737/RDS-2024-0012.
- [49] G.L. Feyisa, K. Dons, H. Meilby, Efficiency of parks in mitigating urban heat island effect: an example from Addis Ababa, Landsc. Urban Plann. 123 (2014) 87–95, https://doi.org/10.1016/j.landurbplan.2013.12.008.
- [50] A. Middel, V.K. Turner, F.A. Schneider, Y. Zhang, M. Stiller, Solar reflective pavements-A policy panacea to heat mitigation? Environ. Res. Lett. 15 (2020) https://doi.org/10.1088/1748-9326/ab87d4.
- [51] R.A. Engel, A. Millard-ball, V.K. Turner, Contributions of roads to surface temperature: evidence from southern California, Environ. Res. Commun. (2022), https://doi.org/10.1088/2515-7620/acabb8.
- [52] J. Yang, E. Bou-Zeid, Designing sensor networks to resolve spatiooral urban temperature variations: fixed, mobile or hybrid? Environ. Res. Lett. 14 (2019) https://doi.org/10.1088/1748-9326/ab25f8.
- [53] L. Romero Rodríguez, J. Sánchez Ramos, F.J. Sánchez de la Flor, S. Álvarez Domínguez, Analyzing the urban heat Island: comprehensive methodology for data gathering and optimal design of mobile transects, Sustain. Cities Soc. 55 (2020), https://doi.org/10.1016/j.scs.2020.102027.
- [54] NOAA, Urban Heat Island Mapping Is Revolutionizing How Cities Address Extreme Heat: Jeremy Hoffman, Ph.D., Reflects on the Origins of This Growing Community Science Movement, 2023, pp. 1–8. https://www.noaa.gov/education/stories/urban-heat-island-mapping-is-revolutionizing-how-cities-address-extreme-heat. (Accessed 23 February 2022).
- [55] A. Ossola, G.D. Jenerette, A. McGrath, W. Chow, L. Hughes, M.R. Leishman, Small vegetated patches greatly reduce urban surface temperature during a summer heatwave in Adelaide, Australia, Landsc. Urban Plann. 209 (2021), https://doi.org/10.1016/j.landurbplan.2021.104046.
- [56] C. Pallai, K. Wesson, Chesapeake Bay Program Partnership High-Resolution Land Cover Classification Accuracy Assessment Methodology, 2017.
- [57] A. Middel, E.S. Krayenhoff, Micrometeorological determinants of pedestrian thermal exposure during record-breaking heat in Tempe, Arizona: introducing the MaRTy observational platform, Sci. Total Environ. 687 (2019) 137–151, https://doi.org/10.1016/j.scitotenv.2019.06.085.